Sustainable Glycerol Terpolycarbonates As Temporary Bioadhesives

SCHOLARONE™
Manuscripts

ARTICLE

Sustainable Glycerol Terpolycarbonates As Temporary Bioadhesives

Anjeza Petersen,[a§] Ngoc-Quynh Chu,[b§] Danielle M. Fitzgerald,[a] Ethan Z. McCaslin,[a] William A. Blessing,[b] Aaron H. Colby,[a] Yolonda L. Colson,[b*] and Mark W. Grinstaff [*a]
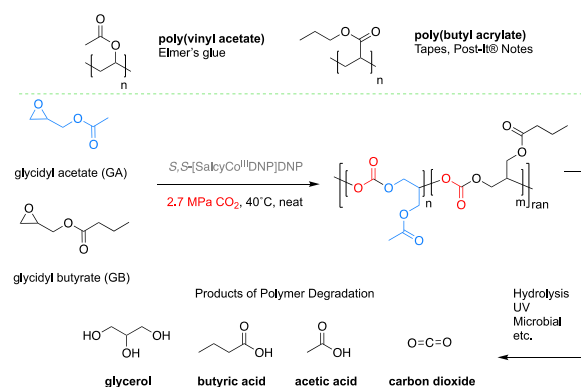
We describe the synthesis of poly(glycidyl acetate-*co*-glycidyl butyrate carbonate)s via the terpolymerization of glycidyl acteate (GA), glycidyl butyrate (GB), and CO_2 by a cobalt salen complex in high atom economy. These new non-cytotoxic polycarbonates are pressure-sensitive adhesives, and peel testing shows the adhesive strength ranges from Scotch-Tape® to hot-melt glues based on glycidyl butyrate content. The tunable adherence, benign degradation products, and facile application and removal suggest their utility as temporary adhesives, such as those used in biomedical applications or medical devices. One polymer, (GA-*co*-GB)-87, exhibits the proper adhesive strength to sufficiently adhere a collagen buttress to the jaws of a steel surgical stapler and easily release the buttress after firing to successfully cut, close, and implant the buttress into lung tissue in an *ex vivo* sheep model.

Introduction

Pressure sensitive adhesives (PSAs) are a class of polymers that adhere dissimilar surfaces under light contact pressure.[1] For medical applications, PSAs are utilized in surgical tapes[2, 3], biomedical electrodes for patient monitoring[4], and transdermal drug delivery systems[5]. They are also employed in surgical devices to temporarily hold an implantable, such as a collagen buttress, in position for subsequent deployment. [6-8] For example, surgeons performing tissue resections (of lung, stomach, colon) reinforce the staple line with a permanent or absorbable buttress to reduce the risk of air or fluid leakage, bleeding, or dehiscence.[9] One of the clinical challenges, however, is aligning and securing the buttress to the stapler to allow division of the tissue and sealing of the staple line concurrently, and then release of the buttress from the stapler without damaging the new anastomosis or surgical resection margin. Both of these steps are critically important to clinical success and in lowering operative morbidity and mortality.

To date, implemented solutions include designs of complex "tear-away" polymer sleeves placed over the anvil of the stapler or stapler-to-buttress adhesives that fasten the collagen buttress to the jaws of the surgical stapler before firing. Strong adhesives such as cyanoacrylates[10] have been explored with minimal clinical adoption given the known toxicity[11] and the significant difficulty in separating the buttress from the stapler after firing which increases the likelihood of a leak or bleeding due to tearing of the staple line and nearby fragile tissue. Thus, weaker adhesives, such as aqueous solutions of cellulose derivatives, are being used with better biocompatibility. These adhesives are sufficiently tacky but must be applied expeditiously prior to stapler-firing due to time-dependent loss of adhesion during wetting, which increases the likelihood for the buttress to shift during stapler positioning and misalignment after stapler firing.[12]

Figure 1. Chemical structures of two common adhesives: poly(vinyl acetate) and poly (butyl acrylate). Synthetic scheme to poly(glycidyl acetate-*co*-glycidyl butyrate carbonate) (GA-*co*-GB) via the terpolymerization of glycidyl acetate (GA), glycidyl butyrate (GB), and CO_2 catalyzed by a salen-cobalt(III) complex. The degradation products and reactants complete a sustainable lifecycle.

a. Departments of Chemistry, Biomedical Engineering, and Medicine, Boston University, Boston, MA, 02215, USA.
b. Division of Thoracic Surgery, Massachusetts General Hospital, Harvard Medical School, Boston, MA, 02114, USA.
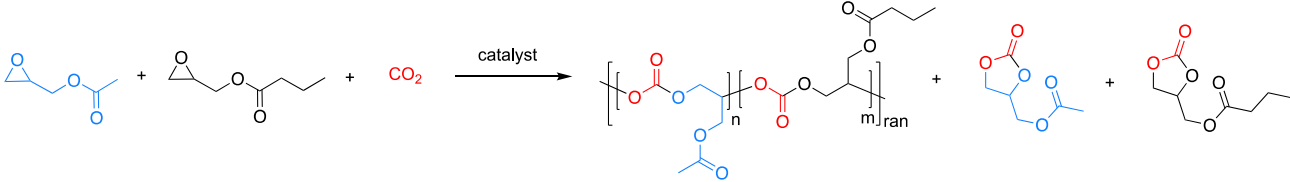
Therefore, the design criteria for a buttress adhesive to achieve sufficient buttress alignment without cumbersome detachment from the anvil of the stapler includes temporary sufficient adhesion, biocompatible, bioresorbable, nonvolatile, and degradable. Further, applying the adhesive without the need for heat or organic solvents, and the adhesive possessing tunable adhesion properties are added benefits to clinical translation. Towards this goal, we disclose the synthesis of a series of new terpolycarbonates as pressure sensitive adhesives with controllable adhesion properties. Inspired by the chemical substructure of non-toxic commercial adhesives (Figure 1), and with the goal of sustainability in mind, we chose monomeric reactants with bio-derived feedstocks such as glycerol. Glycerol-based polymers are finding ever increasing uses.[13-19] It is important to note that currently glycerol is derived from petroleum feedstocks as a bio-based supply chain does not yet exist, but the development and implementation is currently being discussed and pursued.[20] Bio-derived monomers such as limonene oxide[21], castor oil[22], and tricyclic anhydride[23], are increasingly used to generate novel polymeric pressure sensitive adhesives. Additionally, the transformation of gaseous carbon dioxide, a greenhouse gas, into the described adhesive contributes to the sustainability of the synthesis. From a biocompatibility design perspective, we also recognize the need to consider the products of polymer decomposition and, therefore, we judiciously chose materials whose degradation products are known to be safe, are on the FDA Generally Recognized as Safe (GRAS) list, or are fit for human consumption (Figure 1).[24-26]
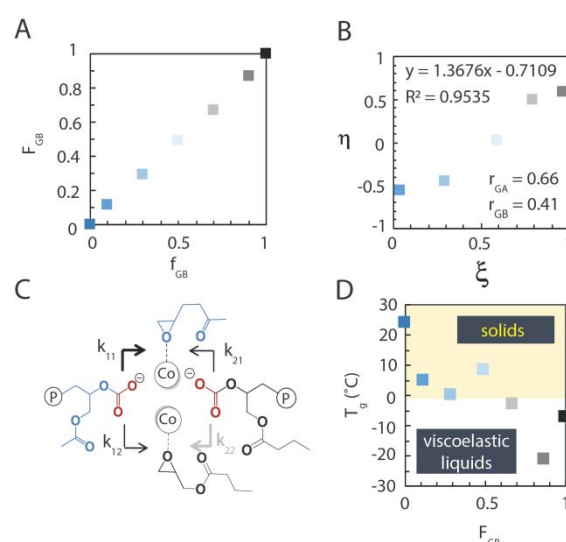
Results and discussion

We used a green synthetic pathway incorporating glycerol-derived oxiranyl monomers and carbon dioxide, catalyzed by an organometallic complex, to produce a carbonate copolymer perfectly alternating in architecture between CO_2 and epoxide monomer. This synthetic methodology was first reported by Inoue et al.[27] and optimized by Lu et al.[28], with low-loading of a highly efficient salen-cobalt(III) catalyst that demonstrates high selectivity for polymer over cyclic carbonate byproduct. Furthermore, this catalyst can efficiently be removed from the polymer product via resuspension in methanol and recycled for re-use. Organometallic

Figure 2. A Composition diagram for terpolymerization of GA with GB and CO_2. B. Kelen-Tudos plot of GA/GB/CO_2 terpolymerization. (See SI Table S1 for full computational analysis). C All possible reaction propagation pathways. D Glass transition temperature of all materials vs. % GB incorporation in polymer chain.

catalysts are widely used for this type of polymerization and accommodate various epoxide monomers[29-41] (SI Table S2), allowing for the fine-tuning of the polymer composition and microstructure to attain desired performance properties.

Specifically, we synthesized poly(glycidyl acetate-co-glycidyl butyrate carbonate) (GA-co-GB) via the terpolymerization of glycidyl acetate (GA), glycidyl butyrate (GB), and 2.7 MPa of CO_2 catalyzed by a cobalt salen complex (2000:1 catalyst loading) at 40 °C (Figure 1). The ester alkyl side chain of glycidyl butyrate imparts adhesivity through van der Waals interactions, while glycidyl acetate raises polymeric cohesive strength by tighter compaction of polymer chains. We previously reported the hydrolytic degradation of glycerol carbonates through the polymer's carbonate linkages.[32]

Table 1. CO_2/GA/GB terpolymerization mediated by (S,S)-[SalcyCo^{III}DNP]DNP

Entry	Feed[a]	Time (h)	GB linkages (mol %) [b]	TOF (h⁻¹) [c]	Selectivity (%) [d]	M_n (Kg/mol) [e]	Đ [e]	T_g (°C)[f]
PGBC-100	GB	24	100	74	85	12.4	1.20	-7
(GA-co-GB)-87	GA/GB(1/9)	24	87	58	96	18.9	1.15	-21
(GA-co-GB)-67	GA/GB(3/7)	16	67	102	91	17.8	1.17	-3
(GA-co-GB)-49	GA/GB(5/5)	12	49	112	94	17.2	1.16	8.5
(GA-co-GB)-29	GA/GB(7/3)	7	29	142	88	11.6	1.21	0
(GA-co-GB)-12	GA/GB(9/1)	6	12	140	87	12.1	1.14	5
PGAC-100	GA	6	0	164	99	13.3	1.13	25

[#]The reaction was performed in neat epoxide (10 mmol) in a 15 mL autoclave under 2.7 MPa CO_2 pressure at 40 °C with 2000:1 catalyst loading. [a] Molar ratio [b] Percent incorporated in polymer as determined by NMR [c] Turnover frequency (TOF) = [mole of product (polycarbonates + cyclic carbonates)]/[mol of starting materials]*[mol of cat per hour]. [d] Percent of polymer formed vs. cyclic carbonate as determined by ^1H NMR [e] Determined by gel permeation chromatography (GPC) in THF, calibrated with polystyrene standards [f] Determined by DSC analysis.

The decomposition products of the (GA-*co*-GB) terpolymers discussed herein are benign: glycerol, a food additive identified as GRAS by the FDA; butyric acid, a compound responsible for the sharp order of feta cheese; acetic acid, a major compound in vinegar; and CO_2, an atmospheric gas (Figure 1).

We prepared a small library of new polymers with varying monomeric feed ratios of glycidyl acetate (GA), and glycidyl butyrate (GB) to characterize the polymer reaction as well as to prepare materials for structure-property analysis (Table 1). The catalyst polymerized GA with high turn-over frequency (TOF, 164 h^{-1}), high polymer selectivity (>99%), moderate molecular weight (13.3 kg/mol), and low dispersity (1.13). Under the same conditions,

The glass transition temperature, as measured by differential scanning calorimetry, is 25°C and -7°C for poly GA and poly GB, respectively. As GB content in the polymer increases, the glass transition decreases from 5 to -21°C. The T_g of (GA-*co*-GB)-87 is lower than PGBC-100, likely due to the differences in molecular weight, with the higher molecular weight (GA-*co*-GB)-87 exhibiting a lower T_g. Three of the formulations, PGBC-100, (GA-*co*-GB)-87, and (GA-*co*-GB)-67 are viscous liquids at room temperature and are therefore appropriate adhesion materials for evaluation (Figure 2E).

Next, we determined the adhesive force of these terpolymers using 180° peel testing (i.e., the force per width required to separate an adhesive-coated flexible substrate from a rigid
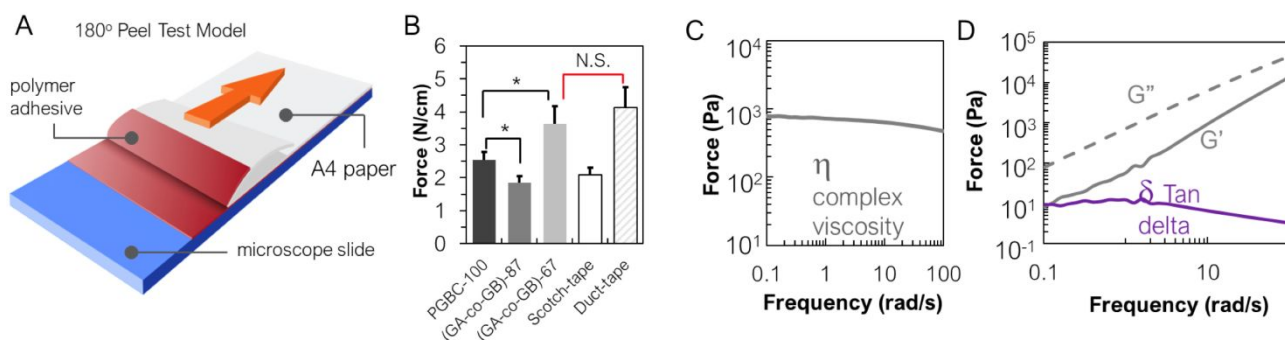
Figure 3. **A** Concept image of peel testing design. **B** Peel testing (180°) of (GA-co-GB) polymers, Duct-Tape®, and Scotch-Tape®, at room temperature (22 ^{o}C) on glass base stock. * Statistically significant (ANOVA P<0.05) N.S.= statistically not significant (ANOVA P>0.05). **C** Frequency sweep (1 % strain, 25 ^{o}C) of the complex viscosity of (GA-co-GB)-87. **D** Frequency sweep (1 % strain, 25 ^{o}C) of the Storage (G') and Loss (G") modulus of (GA-co-GB)-87.

the catalyst polymerized GB with lower TOF (74 h^{-1}), lower polymer selectivity (85%), similar molecular weight of (12.4 kg/mol), and similar dispersity (~1.2). In the CO_2/GA/GB terpolymerization, increased GA monomer feed percentages led to sequentially higher TOFs compared to GB alone. ICP-MS analysis confirmed the removal of residual cobalt from the terpolymer, as the cobalt level was below the limit of detection of the method (SI Figure S7).

We observed a bimodal distribution of chain length for most polymers by GPC analysis, while dispersities remained low at ~1.2 (SI Figure S8). This observable phenomenon is due to adventitious water molecules, as revealed by MALDI-TOF spectrometry which showed two initiating groups (hydroxyl and dinitrophenoxide) for polymeric chains and one terminating group (hydroxyl) (SI Figure S9).[42] The polymers displaying bimodal distributions were synthesized during high humidity days (<60% RH) and the polymers exhibiting unimodal distributions were synthesized during low humidity days (<35% RH). To confirm the role of adventitious water in the polymerization, we conducted a polymerization on a low humidity day (32% RH) and artificially humidified the vapor inside of the reactor. The GPC trace of this polymer showed a bimodal distribution, with the larger peak representing initiation from water (SI Figure S10).

Analysis of monomer feed ratio to polymer composition shows a strong positive correlation (Figure 2A). We utilized an extended Kelen-Tudos-(high conversion) linearization method[43] to derive the reactivity ratios from the ^{1}H NMR spectra of pure polymers via the peak integration of the two distinct pendant esters (SI Figure S5). Reactivity ratios (r) for GA and GB are 0.66 and 0.41, respectively. Because both ratios are below 1, these results indicate GA and GB slightly prefer cross-propagation during terpolymerizaton, and polymer compositional distribution mirrors feed composition.

substrate; American Society for Testing and Materials D903). We evaluated the relative adhesive strength of viscous polymers PGBC-100, (GA-*co*-GB)-87, and (GA-*co*-GB)-67, as well as Scotch-Tape®, Duct-Tape®, for comparative purposes (Figure 3A). We used glass slides (SiO_2) as the base stock and A4 paper (2.6cm x 8cm) wetted with neat adhesive as the face stock (Figure 3A). Additionally, there is no statistical difference in the adhesive strength of Duct Tape® with commercial backing compared to with A4 paper as the face stock (SI Figure S11).

PGBC-100 exhibits a peel strength of 2.6 ± 0.23 N/cm. Incorporation of 23% GA substituents, (GA-*co*-GB)-87, reduces the peel strength to 1.8 ± 0.18 N/cm, which is comparable to Scotch-Tape® (3M 810; 2.1 ± 0.20 N/cm). Increasing GA content in the terpolymer to 33%, (GA-*co*-GB)-67, significantly raises the peel strength to (3.6 ± 0.55 N/cm), comparable to Duct-Tape® (3M 2929; 4.1 ± 0.48 N/cm; Figure 3B). The increase in adhesive strength with higher %GA content is a result of tighter packing between polymer chains. All polymer adhesives undergo cohesive failure due to weaker bulk forces than surface bonding forces.

While (GA-*co*-GB)-67 possess a stronger adhesive profile, (GA-*co*-GB)-87 exhibits lower viscosity and better fluidity. Rheometric testing of this formulation, at a frequency of 0.1 rad/s (Figure 3C) reveals a low complex viscosity of 782 Pa. Additionally, GA-*co*-GB-87 exhibits the lowest T_g of the polymer derivatives, confirming that it is the most fluid, reflecting the ability of the longer alkyl pendant chains to slide across one another. Oscillatory frequency sweeps of (GA-*co*-GB)-87 indicate non-Newtonian behavior with higher flow than elastic deformation (Figure 3D). We selected (GA-*co*-GB)-87 for this surgical application because it can be easily spread onto a collagen surface without the need of solvents or heat, while also demonstrating sufficient adhesive strength to keep the buttress in place.

Given that (GA-*co*-GB)-87 exhibits the desired profile (adhesion and low viscosity), we evaluated the cytotoxicity and immunogenicity of the polymer using an MTS assay and ELISA assay respectively. (GA-*co*-GB)-87 is non-cytotoxic to NIH 3T3 fibroblasts at low doses and minimally cytotoxic at the highest concentration (SI Figure S12). (GA-*co*-GB)-87 is also non-immunogenic to RAW 264.7 macrophages (ATCC TIB-71; SI Figure S13).

Next, we assessed the degradation profile of (GA-*co*-GB)-87 in phosphate buffered saline (PBS) or PBS with added cholesterol esterase at 37 ˚C. The molecular weight of the polymer was monitored via GPC at 2 days, 1 week, 2 weeks, and 3 weeks of incubation. In the PBS and PBS with esterase treatment groups, a new lower molecular weight peak appeared in the GPC trace as a function of time (SI Figure S14A, B, and C). The molecular weight of this polymer is approximately 30% smaller than the original polymer. The dispersity of this polymer also increased over time, consistent with further degradation of the polymer. By day 21, about 50% of the original polymer had degraded. Degradation was
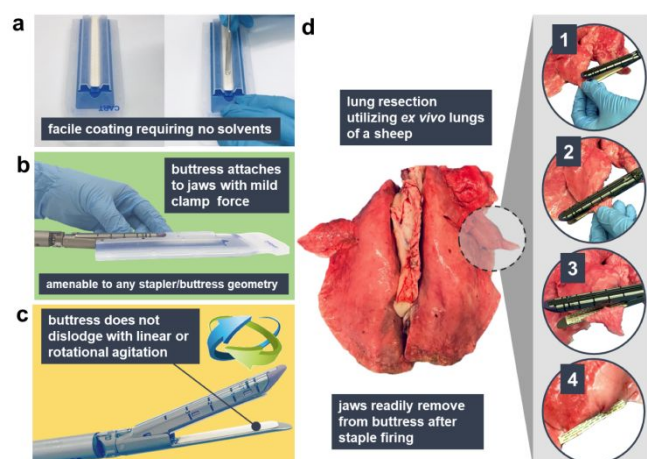
Figure 4. A Coating of (GA-*co*-GB)-87 adhesive to bovine pericardium collagen buttress. **B** Attachment of the adhesive coated collagen buttress to the jaws of a surgical stapler and removal from the manufacture packaging. **C** Continual agitation, rotation, and closing/opening of the surgical stapler does not detach the buttress from the jaws. **D** Surgical resection of lung tissue using the adhesive coated collagen buttress attached to the surgical stapler. After stapler firing, the buttress incorporates in the staple line and easily detaches from the jaws when the stapler is open, requiring no additional manoeuvres to release the tissue from the stapler.

not increased in the presence of the esterase and was slightly less. Future studies will investigate the degradation mechanism as well as the residence time when implanted *in vivo*.

Finally, we evaluated its performance as an adhesive for attachment of a collagen buttress to a surgical steel stapler. When implanted, buttresses provide reinforcement at the staple line to prevent complications related to leakage of air or intraluminal fluid through the staple line that can lead to significant morbidity and even death. We assessed the efficacy of the adhesive to resect a portion of *ex vivo* lung tissue using four criteria. First, the stapler line cartridge surface binds the (GA-*co*-GB)-87 coated collagen by the usual force that is applied with normal closure of the stapler as the buttress is "grabbed" between the jaws of the stapler to remove it from its packaging. Second, maneuvering the tissue

between the jaws of the stapler to the site of resection does not detach the buttress. Third, after stapler firing, the collagen buttress remains attached to the tissue in line with the staple line and easily detaches from the stapling device upon opening of the jaws without need for additional intervention that could force undue errors such as tearing the buttress or incurring additional trauma to the underlying tissue. Finally, adequate closure of the tissue resection margin without air leaks at the site of the staple line.

We coated the collagen buttress (bovine pericardium, PERI-STRIP DRY®, Synovis) without the aid of solvents or heat (SI Figure S15A; Movie 1) by applying a thin layer (≈0.5 mm) of (GA-*co*-GB)-87 to the buttress using a spatula. As shown in SI Figure S15B (movie 2), the stapler jaws (ENDO GIA™ Ultra universal 12mm stapler and ENDO GIA™ 45mm articulating tri-staple reload, Medtronic) bind to and release the buttress from the packaging after application of a mild force to close the jaws of the stapler. Motions of sequential jaw closing/opening and rotation does not detach the buttress from the device (SI Figure S15C; Movie 3). After the stapler is fired, the staples secure the buttress to the tissues allowing separation of the buttress from the jaws of the stapler simply by opening the stapler (SI Figure S15D; Movie 4). Lastly, no air leaks (absence of bubbles) are observed when the resected lung tissue is submerged under water and sequentially inflated/deflated (25 cm of water) for 5 trials. The encouraging results above support future evaluation of this adhesive coated buttress and surgical stapler in an *in vivo* large animal lung resection model.

Conclusion

Cobalt(III) salen catalyzed terpolymerizaton of CO_2, glycidyl acetate (GA), and glycidyl butyrate (GB), affords a series of new polycarbonates with high efficiency. Of the synthesized polymers, (GA-*co*-GB)-87 and (GA-*co*-GB)-67 are pressure sensitive adhesives with peel strengths comparable to Scotch-Tape® and Duct-Tape®, respectively. Neat (GA-*co*-GB)-87 flows readily at room temperature and is a temporary adhesive for use with a surgical stapler as demonstrated by successful implantation of a collagen buttress and closure of an *ex vivo* sheep lung resection margin. With a CO_2 sequestration-based polymer synthesis, benign degradation products after chain scission, and tuneable adhesion, these terpolymers will be of interest for a variety of clinical uses that require temporary and specifically tailored adhesive strength.

Experimental

General Information
All manipulations involving air- and/or water-sensitive compounds were carried out in a glovebox. All oxiranyl monomers were refluxed over CaH_2, and fractionally distilled under a nitrogen atmosphere prior to use. Carbon dioxide (99.995%, bone dry) was purchased from Airgas and used as received. Reagents were purchased from Sigma Aldrich and used as received. All measurements were taken from distinct samples.

NMR experiments
^{1}H and ^{13}C NMR spectra were recorded on a Varian 500 MHz type (^{1}H, 500MHz; ^{13}C, 125 MHz) spectrometer. Their peak frequencies were referenced against the solvent, chloroform-d, at δ 7.24 for ^{1}H NMR and δ 77.23 ppm for ^{13}C NMR, respectively.

Gel Permeation Chromatography

All polymer molecular weights were determined by gel permeation chromatography versus polystyrene standards (Agilent Technologies) using THF as the eluent at a flow rate of 1.0 mL/min through a Styragel column (HR4E THF, 7.8 x 300 mm) with a Waters 2414 refractive index detector.

MALDI-ToF

MALDI-ToF mass values for polymers were determined using a Bruker autoflex Speed MALDI-ToF mass spectrometer equipped with a SMART-beam II and a flash detector. Samples were prepared by dissolving in a 1:1 vol/vol mixture of matrix solvent (10 mg/mL solution of dithranol in THF with 0.1% AgTFA) and 10 mg polymer dissolved in minimal amount THF.

Differential Scanning Calorimetry

The thermal properties of the polymers were measured by Differential Scanning Calorimetry (DSC) using a TA Q 100 under a nitrogen atmosphere (nitrogen flow rate: 60 mL min^{-1}). All samples were tested at a heating rate of 10°C/min and a cooling rate of 10 °C/min from -40 to 80°C. The weight of all samples was between 2 to 10 mg and the samples underwent three heat-cool-heat cycles. The glass transition temperature, T_g, was noted in the DSC-thermogram as the midpoint temperature of the glass transition peak in the second heating cycle (Supplementary Fig. 9).

ICP-MS

Residual cobalt in the polymer was detected via ICP-MS (Inductively Coupled Plasma-Mass Spectrometer) (Thermo VG PQ ExCell). Standards were prepared using a purchased 1000 μg/mL Co solution in 2% nitric acid (High-Purity Standards, #100013-1) 0.001 to 1 ppb. (GA-co-GB)-87 sample was taken following the reaction workup in methanol and diluted using 2% nitric acid solution to 1 ppb. The limit of detection (LOD) was calculated from the average of 4 blank values of 2% nitric acid solution using the following equation: LOD = blank average + (3*blank standard deviation), LOD signal = 2026.771. The (GA-co-GB)-87 sample was injected twice on the ICP-MS and the detected Co was below the LOD (sample signals: 1925.13 and 1747.295).

180° Peel Strength

The peel adhesion test was carried out at room temperature (22°C) by using Fischerbrand glass microscope (SiO$_2$) slides (base stock) and a A4 paper (face stock) as substrates.

The face dimensions for the glass slides were 7.6 cm × 2.6 cm. The adhesive was coated on the non-frosted surface of the glass plate containing a coating area of 2 cm × 2.6 cm with a coating thickness of ~30 μm. Then, the paper substrate was stuck on the coated glass slide with moderate human finger pressure. The sample was let to settle for 1 minute prior to testing on an Intron 5944 with peel speed operating at 360 mm/min.

Commercial all-purpose Duct Tape® (3M 2929) and Scotch Tape® (3m 810) were used as received, (besides width modifications) and stuck to the glass. Duct tape was cut to 2.6 cm of width, scotch tape was not modified. Three separate specimens were used for each adhesive formulation in this test. The average peak from the load propagation graph was used to calculate the peeling force. Peel strength is defined as the average load per width of the bondline required to separate progressively a flexible member from a rigid member (ASTM D 903).

Probe Tack

All tack testing were performed on a Discovery Hybrid Rheometer (DHR-2 series) with 8 mm stainless steel-sand blasted parallel plate geometry with a Peltier plate. The adhesive was placed on the bottom plate and a top probe moving at 100 ⬚m/sec rested on the adhesive until the desired axial force was reached. After 5 seconds, the top probe pulled away at a rate of 100 ⬚m/sec.The peak of the force curve is defined as the tack strength (T_s) and the area under the curve is defined as the tack energy (T_e) as calculated by eq. (1), where A denotes the surface area (m^2) of the probe, r is the rate of probe separation in debonding (m/s), F is the force (N) measured during debonding, and t is the time in seconds;

$$T_e = 2 \ x\left[\frac{r}{A}\int_{ti}^{tf}F(t)dt\ \right] \quad\quad (1)$$

Frequency Sweeps

All oscillatory sweeps were performed on a Discovery Hybrid Rheometer (DHR-2 series) with 8 mm stainless steel parallel plate geometry with a gap size of 50 ⬚m. Frequency sweeps were performed from 0.1 to 100 rad/s or 1 to 500 rad/s at 1% strain (determined to be in the linear viscoelastic region with a previous strain sweep) at specified temperatures (20°C, 25°C, 37°C, 50°C) controlled by a Peltier plate.

Cell Culture

NIH 3T3 murine fibroblasts (ATCC) were cultured in Dulbecco's modified Eagle's medium supplemented with 10% bovine calf serum and 1% penicillin-streptomycin. RAW 264.7 murine macrophages (ATCC) were cultured in Dulbecco's modified Eagle's medium supplemented with 10% fetal bovine serum and 1% penicillin-streptomycin. Cells were maintained in a sterile, humidified environment at 37 °C with 5% CO$_2$.

In Vitro Evaluation of Cytotoxicity

NIH 3T3 cells were seeded in a 96-well plate at a density of 20,000 cells/well and were allowed to adhere for 24 h. The media was then replaced with fresh media, and cells were incubated with polymer samples in 5% DMSO using transwell inserts (0.4 μm pores). Cell viability was assessed 24 h after treatment via the MTS in vitro cytotoxicity assay (CellTiter 96 Aqueous One, Promega). The average of two experiments (N=2) in which n=6 per polymer concentration.

In Vitro Evaluation of Immunogenicity

RAW 264.7 cells were seeded in a 96-well plate at a density of 30,000 cells/well and were allowed to adhere for 24 h. The media was then replaced with fresh media, and cells were incubated with polymer samples in 5% DMSO using transwell inserts (0.4 μm pores). IL-6 levels were measured via ELISA kit (Abcam) and compared to those of RAW 264.7 treated with lipopolysaccharide—a molecule known to stimulate IL-6 production and immunogenicity *in vitro* (n=6)*.

Degradation Study

The degradation profile of (GA-*co*-GB)-87 was assessed in phosphate buffered saline (PBS) or PBS and cholesterol esterase. Approximately 30mg of (GA-co-GB)-87 polymer was weighed onto a 9x9 mm glass coverslip (COVERGLASS #72190-09) and placed into a 12-well Transwell plate. 2 mL of PBS was added to each well. In the enzyme treatment groups, 20U of cholesterol esterase was added to each well. The Transwell plate was placed in an incubator at 37˚C, 5% CO$_2$ and underwent moderate shaking throughout the duration of the experiment. Aliquots of the media were removed at days 2, 7, 14, and 21 and stored at -80˚C. Each week, an additional 5U of enzyme were added to the treatment groups to maintain esterase activity. Following storage, samples were prepared at 1 mg/mL concentration in nitrate buffer for analysis on an aqueous GPC against polyethylene glycol standards.

Representative Polymer Synthesis

In a glovebox, glycidyl butyrate (0.67 mL, 5 mmol) glycidyl acetate (0.51 mL, 5 mmol) were added into a high pressure autoclave, followed by the addition of *(S,S)*-SalcyCo^{III}DNP (5.21 mg, 0.005 mmol). The autoclave was transferred out of the glovebox and

charged with CO_2 to 2.7 MPa. The reaction was allowed to run at 40 °C for 10 hr. Subsequently, the reaction vessel was placed in an ice bath for 10 minutes and the CO_2 pressure was released. The reaction mixture was diluted in minimal amount DCM. The mixture was added dropwise into cold MeOH (50 ml) and the precipitated polymer was collected. The precipitation was repeated for a total of 3 times until complete removal of the catalyst and unreacted monomer. The resultant material was dried under vacuum to yield ~ 300 mg of a viscous liquid/brittle solid. Please see the ESI for complete characterization details for all of the polymers.

Conflicts of interest

There are no relevant conflicts to declare.

Acknowledgements

  *Corresponding Authors: Mark W. Grinstaff   mgin@bu.edu and Yolonda L. Colson ycolson@mgh.harvard.edu

§ Co-first authors

ORCID

Anjeza Petersen	0000-0003-4686-8123
Ngoc-Quynh Chu	0000-0003-0042-0833
Ethan Z. McCaslin	0000-0001-6129-1559
Danielle M. Fitzgerald	0000-0001-7158-0522
William A. Blessing	0000-0002-3145-7762
Aaron H. Colby	
Yolonda L. Colson	0000-0002-8229-5636
Mark W. Grinstaff	0000-0002-5453-3668

Notes and references

1.   C. Creton, *MRS Bulletin*, 2003, **28**, 434-439.
2.   I. Webster, *International Journal of Adhesion and Adhesives*, 1999, **19**, 29-34.
3.   *United States Pat.,* US 3,121,021, 1964.
4.   A. K. Zbigniew Czech, Jolanta Swiderska, in *Wide Spectra of Quality Control*, ed. I. Akyar, Books on Demand, 2011, ch. 17, p. 546.
5.   M. R. Prausnitz and R. Langer, *Nature Biotechnology*, 2008, **26**, 1261-1268.
6.   *United States Pat.,* US 7,780,685 B2, 2010.
7.   *United States Pat.,* US 6,592,597 B2, 2003.
8.   *United States Pat.,* US 7,708,180 B2, 2010.
9.   L. S. F. Yo, L. S. F. Yo, E. C. J. Consten, E. C. J. Consten, H. M. E. Quarles Van Ufford, H. M. E. Quarles Van Ufford, H. G. Gooszen, H. G. Gooszen, M. Gagner and M. Gagner, 2006, **23**, 283-291.
10.   *United States Pat.,* US 5,441,193, 1995.
11.   R. T. Moretti Neto, I. Mello, A. B. D. S. Moretti, C. R. C. Robazza and A. A. C. Pereira, *Brazilian Oral Research*, 2008, **22**, 43-47.
12.   *United States Pat.,* US 5,752,965 A, 1998.
13.   N. G. Ricapito, C. Ghobril, H. Zhang, M. W. Grinstaff and D. Putnam, *Chemical Reviews*, 2016, **116**, 2664-2704.
14.   F. Zabihi, H. Koeppe, K. Achazi, S. Hedtrich and R. Haag, *Biomacromolecules*, 2019, **20**, 1867-1875.
15.   P. N. Zawaneh, S. P. Singh, R. F. Padera, P. W. Henderson, J. A. Spector and D. Putnam, *Proceedings of the National Academy of Sciences*, 2010, **107**, 11014-11019.
16.   Y. X. Bowen Xiang, Zhiyong Liu, Jia Tian, Holger Frey, Yun Gao, Weian Zhang, *Polymer Chemistry*, 2020, **11**, 3913-3921.
17.   H. Zhang and M. W. Grinstaff, *Macromolecular Rapid Communications*, 2014, **35**, 1906-1924.
18.   W. C. Ray and M. W. Grinstaff, *Macromolecules*, 2003, **36**, 3557-3562.
19.   M. A. Carnahan and M. W. Grinstaff, *Macromolecules*, 2001, **34**, 7648-7655.
20.   C. L. Gargalo, A. Carvalho, K. V. Gernaey and G. Sin, *Industrial & Engineering Chemistry Research*, 2017, DOI: 10.1021/acs.iecr.7b00908, 6711-6727.
21.   T. T. D. Chen, L. P. Carrodeguas, G. S. Sulley, G. L. Gregory and C. K. Williams, *Angewandte Chemie International Edition*, 2020, **59**, 23450-23455.
22.   S. Lee, K. Lee, Y.-W. Kim and J. Shin, *ACS Sustainable Chemistry & Engineering*, 2015, **3**, 2309-2320.
23.   N. J. Van Zee and G. W. Coates, *Angewandte Chemie International Edition*, 2015, **54**, 2665-2668.
24.   CPG Sec 562.100 Acetic Acid - Use in Foods - Labeling of Foods in Which Used, ttps://www.fda.gov/regulatory-information/search-fda-guidance-documents/cpg-sec-562100-acetic-acid-use-foods-labeling-foods-which-used (accessed March 1 2020).).
25.   C. Efthymoiu, *Department of Biology St. John's University*, 1967, 20-24.
26.   A. Beharaj, E. Z. McCaslin, W. A. Blessing and M. W. Grinstaff, *Nature Communications*, 2019, **10**, 1-7.
27.   S. K. Inoue, Hideomi; Tsuruta, Teiji, *Journal of Polymer Science*, 1969, **7**, 287-292.
28.   X.-B. Lu and D. J. Darensbourg, *Chem. Soc. Rev.*, 2012, **41**, 1462-1484.
29.   A. J. Kamphuis, F. Picchioni and P. P. Pescarmona, *Green Chemistry*, 2019, **21**, 406-448.
30.   S. J. Poland and D. J. Darensbourg, *Green Chem.*, 2017, **19**, 4990-5011.
31.   T. Ohkawara, K. Suzuki, K. Nakano, S. Mori and K. Nozaki, *Journal of the American Chemical Society*, 2014, **136**, 10728-10735.
32.   A. Beharaj, I. Ekladious and M. W. Grinstaff, *Angewandte Chemie International Edition*, 2019, **58**, 1407-1411.
33.   C. Martín and A. W. Kleij, *Macromolecules*, 2016, **49**, 6285-6295.
34.   H. Zhang, X. Lin, S. Chin and M. W. Grinstaff, *Journal of the American Chemical Society*, 2015, **137**, 12660-12666.
35.   G. S. Sulley, G. L. Gregory, T. T. D. Chen, L. Peña Carrodeguas, G. Trott, A. Santmarti, K.-Y. Lee, N. J. Terrill and C. K. Williams, *Journal of the American Chemical Society*, 2020, **142**, 4367-4378.
36.   A. Thevenon, A. Cyriac, D. Myers, A. J. P. White, C. B. Durr

and C. K. Williams, *Journal of the American Chemical Society*, 2018, **140**, 6893-6903.

37. F.-T. Tsai, Y. Wang and D. J. Darensbourg, *Journal of the American Chemical Society*, 2016, **138**, 4626-4633.
38. C. M. Byrne, S. D. Allen, E. B. Lobkovsky and G. W. Coates, *JACS Communications*, 2004, **126**, 11404-11405.
39. L. Kunze, S.-Y. Tseng, R. Schweins, T. Sottmann and H. Frey, *Langmuir*, 2019, **35**, 5221-5231.
40. D. J. Darensbourg and S. J. Wilson, *Journal of the American Chemical Society*, 2011, **133**, 18610-18613.
41. Z. Qin, C. M. Thomas, S. Lee and G. W. Coates, *Angewandte Chemie International Edition*, 2003, **42**, 5484-5487.
42. G.-P. Wu and D. J. Darensbourg, *Macromolecules*, 2016, **49**, 807-814.
43. T. T. Kelen, F., *React Kinet Catal Lett*, 1974, **1**, 487-492.